AIMS Mathematics, 9(11): 30781–30815.
DOI:10.3934/math.20241487
Received: 25 August 2024
Revised: 24 September 2024
Accepted: 30 September 2024
Published: 30 October 2024

https://www.aimspress.com/journal/Math

Research article

Optimised block bootstrap: an efficient variant of circular block bootstrap method with application to South African economic time series data

James Daniel[1,*], Kayode Ayinde[2], Adewale F. Lukman[3], Olayan Albalawi[4], Jeza Allohibi[5] and Abdulmajeed Atiah Alharbi[5]

[1] Department of Statistics, Federal University of Technology, Akure, Nigeria

[2] Northwest Missouri State University, Maryvile, USA

[3] Department of Mathematics and Statistics, University of North Dakota, Grand Forks, North Dakota, USA

[4] Department of Statistics, Faculty of Science, University of Tabuk, Tabuk, Saudi Arabia

[5] Department of Mathematics, Faculty of Science, Taibah University, Al-Madinah Al-Munawara 42353, Saudi Arabia

* **Correspondence:** Email: futathesis@gmail.com; Tel: +2348033147591.

Abstract: This study introduced the optimized block bootstrap (OBB), a novel method designed to enhance time series prediction by reducing the number of blocks while maintaining their representativeness. OBB minimized block overlap, resulting in greater computational efficiency while preserving the temporal structure of data. The method was evaluated through extensive simulations of autoregressive moving average (ARMA) models and South Africa economic data which included inflation rates, gross domestic product (GDP) growth, interest rates, and unemployment rates. Results demonstrated that OBB consistently outperformd circular block bootstrap (CBB), providing more accurate forecasts with lower root mean square error (RMSE), which assessed variance, and lower mean absolute error (MAE), which measured bias, across various time series models and parameter settings. Consequently, the OBB method was applied to forecasting of the South Africa economic data, extending up to 2027. The novel approach presented by OBB offered a valuable tool for improving predictive accuracy in time series forecasting, with potential applications across diverse fields such as finance and environmental modeling.

Keywords: bootstrap method; autoregressive moving average (ARMA); measures of accuracy; circular block bootstrap (CBB); optimised block bootstrap (OBB)
Mathematics Subject Classification: 62F40

1. Introduction

In statistical analysis, conventional approaches often employ probabilistic sampling to derive inferences by selecting samples from a sizable population, usually conducted without replacement. Conversely, the concept of bootstrap methodology presents an inverse perspective on sampling.

Bootstrap entails working with a limited set of recorded observations referred to as a surrogate population and repeatedly resampling the small dataset with replacement a significant number of times [11]. This resampling process is instrumental in uncovering and estimating unknown population characteristics by leveraging the information within the bootstrapped samples [31]. The concept of bootstrap was formally introduced and subsequently popularized in [6]. [24] refuted the popular thought on bootstrap's ability to handle any distribution when it categorically pointed out that bootstrap, as introduced in [6], can only handle independent identical distribution (i.i.d.) data and not dependent data. Bootstrap, as introduced in [6], will be referred to as the i.i.d. bootstrap for further discussion.

The i.i.d. bootstrap is not appropriate for dependent data because it disrupts the serial correlation property of the data [2, 27]. The block bootstrap approach is a commonly employed technique in the field of time series analysis to exploit the advantages of the bootstrap technique [14, 30]. The purpose of defining the block bootstrap method is to maintain the time series dependency structure in a surrogate population [15, 17, 22]. [3, 7, 12] developed this method. They created consecutive data blocks and divided the time series into blocks of individual observation units or estimated residuals. The bootstrap data inside each block is created using the classical i.i.d. bootstrap. At the beginning of block bootstrap development, two possible approaches to forming blocks appeared: the nonoverlapping and the overlapping block bootstrap.

The nonoverlapping and overlapping block bootstrap methods pose edge effect problems. While the nonoverlapping block bootstrap category is edge-locked, the overlapping block bootstrap category is not edge-locked, which creates issues. To address this, an improvement was made. The circular block bootstrap (CBB) was developed to mitigate the limitations of overlapping block bootstrap methods by reducing bias near the boundaries of the data. This method provides more accurate estimates, especially when analyzing time series or spatial data.

In CBB, time series data is divided into blocks of consecutive observations; starting from the first block, the process continues in a circular manner, meaning that once the last element is reached, it loops back to the beginning [19, 21]. Although the CBB was developed to solve the edge effect issue in time series data, it generates more blocks compared to traditional block bootstrap methods. Consequently, the performance of CBB can be influenced by the block size, and selecting the optimal block length can be a challenging task [1, 10, 23, 32]. [29] explores the use of deep learning models for prediction refinement, contrasting with this research, which focuses on developing and comparing bootstrap methods to improve time series forecasting accuracy. Both studies emphasize model optimization and performance metrics like the root mean squared error (RMSE); however, while this work is based on statistical resampling techniques, [29] employs neural networks in the context of electric vehicles. Despite their differing methodologies, both studies aim to enhance prediction accuracy and overall model efficiency in their respective domains.

The objective of this paper is to advance a block bootstrap method that will have a moderate number of blocks while still mitigating the edge effect of time series data. This paper extends the CBB method

to a more edge-effect-tolerance block bootstrap method using the autoregressive integrated moving average (ARIMA) model. We also compare CBB with the proposed methods using simulated and real-life data. For constructing the block structure, we use the modulus operation in arithmetic. RMSE and the mean absolute error (MAE) will be used as a comparison measure to assess the performance of the CBB and the proposed method.

The rest of the paper is structured in the following manner. In Section 2, we present a leaner approach to the CBB method with the ARIMA model and describe the steps involved in deriving the block size and its formation. The framework for the proposed method is laid out with the description of univariate time series data described using different variants of the ARIMA technique at different levels of observation sizes, appropriate parameters, and standard deviations. Two accuracy measuring techniques are defined to access accuracy of the proposed and existing methods. In Section 3, we present results of the performance of the two methods as well as that of the real-life data. In Section 4, we provide some concluding remarks.

2. Materials and methods

We consider a time series data given as follows:

$$X_t = x_1, x_2, \cdots, x_n \tag{2.1}$$

Equation (2.1) is obtained from an autoregressive (AR) or moving average (MA) process given as follows.

$$\begin{aligned} X_t =& \mu + \sum_{t=1}^{p} \phi_j X_{t-j} + \sum_{t=1}^{q} \theta_k \varepsilon_{t-k} + \varepsilon_t; \quad \varepsilon_t \sim N(0, \sigma_\varepsilon) \\ \text{for } & \begin{cases} j = 1, 2, \cdots, p; \\ k = 1, 2, \cdots, q; \\ t = 1, 2, \cdots, n; \\ 0 \leqslant |\phi_j| \leqslant 1; \\ 0 \leqslant |\theta_k| \leqslant 1; \\ \phi_j \neq \theta_k; \\ \sum\limits_{t=1}^{n} \varepsilon_t = 0; \\ \varepsilon_t \sim N(0, \sigma^2); \\ \sigma_\varepsilon^2 = \sigma^2; \\ |\mu| \geq 0. \end{cases} \end{aligned} \tag{2.2}$$

2.1. The existing and proposed methods

Hereafter, we refer to n as the time series size. There are many block bootstrap methods for dealing with time series data; of these, we focus on the CBB method based on edge-effect-tolerance ability. In this study we shall be using the CBB as the existing method. The following paragraphs will provide a detailed description of the existing and proposed methods, along with the data simulation procedure.

2.1.1. CBB formation—the existing method

We first describe how to construct CBB blocks based on the ARIMA time series data described in Eqs (2.1) and (2.2). For a given time series $x_1, x_2, \cdots, x_n$, the CBB blocks are constructed as follows.

$$B_\iota = x_{((\iota-1) \mod n)+1}, \cdots, X_{(\iota-1)+\ell \mod n}; \text{ where } \iota = 1, 2, \cdots, n \quad \text{for} \begin{cases} \lim_{\ell, n\to\infty} \frac{\ell}{n} \to \infty; \\ 1 < \ell < n; \\ m = l \end{cases} \tag{2.3}$$

The CBB block is defined in Eq (2.3) as a set of blocks of equal size (ℓ) and equal number of overlap m. Each block consists of consecutive observations of time series data (x_t) described in Eq (2.1) and obtained from an AR or MA process given in Eq (2.2). The blocks formed with this method may be represented as $B_\iota = B_1, B_2, \cdots, B_{n-2}, B_{n-1}, B_n$, where n represent the series size. Illustration of the CBB method as demonstrated by [18] shows that the number of blocks in a CBB block arrangement equals the number of time series observations from which the blocks are formed regardless of its block length. Blocks are formed with extreme observations rebounded to mitigate against the edge-effect while allowing uniform block length in an end-to-start manner.

Figure 1 depicts an illustration for the CBB procedure presented in Eq (2.3). Each arc of the circle (starting from B_1 to B_n) in Figure 1 represents each block of CBB from the time series data X_t. Note that the last three blocks, B_{n-2}, B_{n-1}, and B_n, are supplemented by the first three time series observations x_1, x_2, and x_3 to make each of the blocks a complete block. We refer to it as the CBB due to this reason.

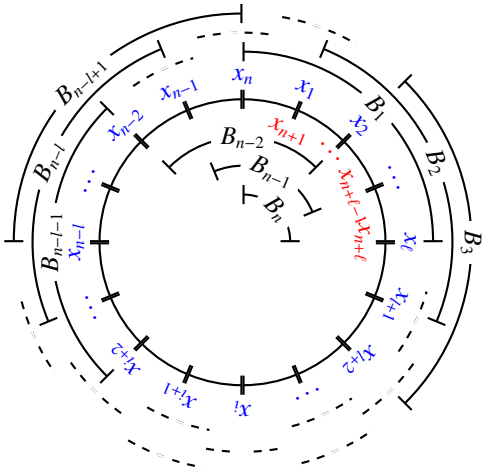

Figure 1. Circular block bootstrap.

If we take an example where $X_t = x_1, x_2, \cdots, x_{12}$ and ℓ equals 4, we can construct the blocks in the following way using Eq (2.3). Let us apply the mathematical formula to the series $x_1, x_2, \cdots, x_{12}$ to obtain each subseries one after the other:

(i) First subseries:

$$\begin{aligned} B_1 &= (x_{(1-1 \mod 12)+1}, \cdots, X_{(1-1 \mod 12)+4}) \\ &= (x_1, x_2, x_3, x_4) \end{aligned}$$

(ii) Second subseries:

$$B_2 = (x_{(2-1 \mod 12)+1}, \cdots, X_{(2-1 \mod 12)+4}) = (x_2, x_3, x_4, x_5)$$

(iii) Third subseries:

$$B_3 = (x_{(3-1 \mod 12)+1}, \cdots, X_{(3-1 \mod 12)+4}) = (x_3, x_4, x_5, x_6)$$

(iv) Fourth subseries:

$$B_4 = (x_{(4-1 \mod 12)+1}, \cdots, X_{(4-1 \mod 12)+4}) = (x_4, x_5, x_6, x_7)$$

(v) Fifth subseries:

$$B_5 = (x_{(5-1 \mod 12)+1}, \cdots, X_{(5-1 \mod 12)+4}) = (x_5, x_6, x_7, x_8)$$

(vi) Sixth subseries:

$$B_6 = (x_{(6-1 \mod 12)+1}, \cdots, X_{(6-1 \mod 12)+4}) = (v_6, x_7, x_8, x_9)$$

(vii) Seventh subseries:

$$B_7 = (x_{(7-1 \mod 12)+1}, \cdots, X_{(7-1 \mod 12)+4}) = (x_7, x_8, x_9, x_{10})$$

(viii) Eighth subseries:

$$B_8 = (x_{(8-1 \mod 12)+1}, \cdots, X_{(8-1 \mod 12)+4}) = (x_8, x_9, x_{10}, x_{11})$$

(ix) Ninth subseries:

$$B_9 = (x_{(9-1 \mod 12)+1}, \cdots, X_{(9-1 \mod 12)+4}) = (x_9, x_{10}, x_{11}, x_{12})$$

(x) Tenth subseries:

$$B_{10} = (x_{(10-1 \mod 12)+1}, \cdots, X_{(10-1 \mod 12)+4}) = (x_{10}, x_{11}, x_{12}, x_1)$$

(xi) Eleventh subseries:

$$B_{11} = (x_{(11-1 \mod 12)+1}, \cdots, X_{(11-1 \mod 12)+4}) = (x_{11}, x_{12}, x_1, x_2)$$

(xii) Twelfth subseries:

$$B_7 = (x_{(12-1 \mod 12)+1}, \cdots, X_{(12-1 \mod 12)+4}) = (x_{12}, x_1, x_2, x_3)$$

The results of the iteration for the CBB blocks are better arranged in a matrix form as follows:

$$B_\iota = \begin{pmatrix} x_1 & x_2 & x_3 & x_4 & & & & & & & & & \mathbf{B_1} \\ & x_2 & x_3 & x_4 & x_5 & & & & & & & & \mathbf{B_2} \\ & & x_3 & x_4 & x_5 & x_6 & & & & & & & \mathbf{B_3} \\ & & & x_4 & x_5 & x_6 & x_7 & & & & & & \mathbf{B_4} \\ & & & & x_5 & x_6 & x_7 & x_8 & & & & & \mathbf{B_5} \\ & & & & & x_6 & x_7 & x_8 & x_9 & & & & \mathbf{B_6} \\ & & & & & & x_7 & x_8 & x_9 & x_{10} & & & \mathbf{B_7} \\ & & & & & & & x_8 & x_9 & x_{10} & x_{11} & & \mathbf{B_8} \\ & & & & & & & & x_9 & x_{10} & x_{11} & x_{12} & \mathbf{B_9} \\ & & & & & & & & & x_{10} & x_{11} & x_{12} & x_1 & \mathbf{B_{10}} \\ & & & & & & & & & & x_{11} & x_{12} & x_1 & x_2 & \mathbf{B_{11}} \\ & & & & & & & & & & & x_{12} & x_1 & x_2 & x_3 & \mathbf{B_{12}} \end{pmatrix} \tag{2.4}$$

Furthermore, each line of the matrix (starting from B_1 to B_{12}) in Eq (2.4) represents each block of the CBB from the time series data described as $X_t = x_1, x_2, \cdots, x_{12}$.

In addition, each arch in Figure 2 represents each line of the matrix (starting from B_1 to B_{12}) in Eq (2.4) from the time series data described in Eq (2.2).

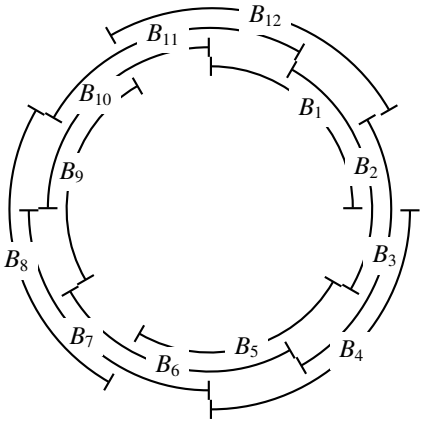

Figure 2. Illustration of CBB.

2.1.2. OBB formation—the proposed method

The CBB involves creating fixed-length blocks. This means that if one needs to use this method, one must choose a block length. If the block length is too small, the CBB cannot capture the chronological order enough. On the other hand, if the block length is too large, the CBB can resample from a few blocks, each with an equally large probability. In CBB, the block length chosen does not determine the number of blocks; rather, the number of blocks is fixed as the number of the observations of the time series denoted by n. Since the sample size is a mater of choice, a moderate number of blocks is required as too many blocks, such as n in the case of CBB leads to a probability that some blocks may escape selection, leading to potential variability in the resampled set. The estimate obtained from a moderate number but not the small of block will better represent its parameter.

The OBB method is a modification of the CBB method from [19]. Given a time series data, $X_t = x_1, x_2, \cdots, x_n$ which follows an AR(p) or MA(q) process summarized in Eq (2.2), the OBB blocks are defined as the blocks of size ℓ consecutive observations starting from x_i as follows.

$$B_\iota = x_{((\iota-1) \mod n)+1}, \cdots, X_{(\iota-1)+\ell \mod n}; \quad \iota = \{x \mid x \in \mathbb{N}, 1 \leq x \leq n, x \mod (\ell+1) \neq 0\} \begin{cases} \lim\limits_{\ell, n\to\infty} \frac{n}{\ell} \to \infty; \\ \iota = 1 \leqq \iota \leq (n - \lfloor \frac{n}{\ell} \rfloor); \\ 1 < \ell < n; \\ m = \ell - 1 \end{cases} \tag{2.5}$$

The OBB block is defined in Eq (2.5) as a set of blocks of equal size (ℓ) with $m = \ell - 1$ number of overlap. Each consist of consecutive observations of time series data (x_ι) described in Eq (2.1) and obtained from an AR or MA process given in Eq (2.2). Equation (2.5) is a modification of Eq (2.3) in a way to reduce the number of overlapping observation from ℓ in the case of CBB to $\ell - 1$, which consequently reduces the number of block by $\lfloor \frac{n}{\ell} \rfloor$. The blocks formed with this method may be represented as $B_\iota = B_1, B_2, \cdots, B_{n-\lfloor \frac{n}{\ell} \rfloor}$, where n represent the series size and ℓ is the block length.

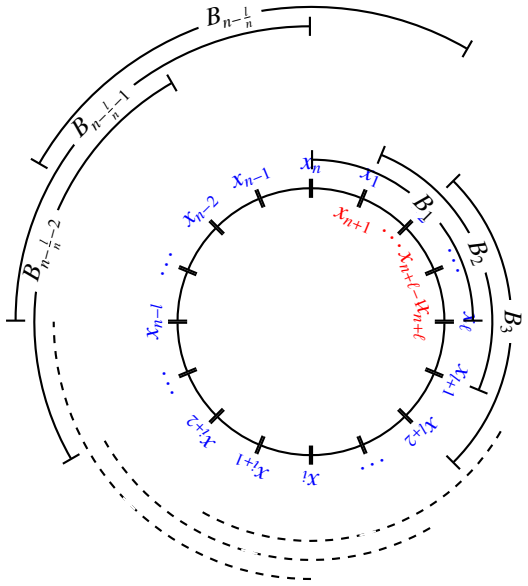

Figure 3. Optimized block bootstrap.

Figure 3 depicts an illustration for the OBB procedure presented in Eq (2.5). Each arc of the circle (starting from B_1 to $B_{n-\lfloor \frac{n}{\ell} \rfloor}$) in Figure 3 represents each block of OBB from the time series data X_t. Reference to the example of $X_t = x_1, x_2, \cdots, x_{12}$, ℓ equals 4, and we can construct the blocks in the following way using Eq (2.5) give $\{x \mid x \in \mathbb{N}, 1 \leq x \leq 12, x \mod 4 \neq 0\}$

(1) First subseries:

$$\begin{aligned} B_1 &= (x_{(1-1 \mod 12)+1}, \cdots, X_{((1-1)+4) \mod 12}) \\ &= (x_1, x_2, x_3, x_4) \end{aligned}$$

(2) Second subseries:

$$\begin{aligned} B_2 &= (x_{(2-1 \mod 12)+1}, \cdots, X_{((2-1)+4) \mod 12}) \\ &= (x_2, x_3, x_4, x_5) \end{aligned}$$

(3) Third subseries:

$$\begin{aligned} B_3 &= (x_{(3-1 \mod 12)+1}, \cdots, X_{((3-1)+4) \mod 12}) \\ &= (x_3, x_4, x_5, x_6) \end{aligned}$$

(4) Fourth subseries:

$$\begin{aligned} B_5 &= (x_{(5-1 \mod 12)+1}, \cdots, X_{((5-1)+4) \mod 12}) \\ &= (x_5, x_6, x_7, x_8) \end{aligned}$$

(5) Fifth subseries:

$$\begin{aligned} B_6 &= (x_{(6-1 \mod 12)+1}, \cdots, X_{((6-1)+4) \mod 12}) \\ &= (v_6, x_7, x_8, x_9) \end{aligned}$$

(6) Sixth subseries:

$$\begin{aligned} B_7 &= (x_{(8-1 \mod 12)+1}, \cdots, X_{((7-1)+4) \mod 12}) \\ &= (x_7, x_8, x_9, x_{10}) \end{aligned}$$

(7) Seventh subseries:

$$\begin{aligned} B_9 &= (x_{(9-1 \mod 12)+1}, \cdots, X_{((9-1)+4) \mod 12}) \\ &= (x_9, x_{10}, x_{11}, x_{12}) \end{aligned}$$

(8) Eighth subseries:

$$\begin{aligned} B_{10} &= (x_{(10-1 \mod 12)+1}, \cdots, X_{((10-1)+4) \mod 12}) \\ &= (x_{10}, x_{11}, x_{12}, x_1) \end{aligned}$$

(9) Ninth subseries:

$$\begin{aligned} B_{11} &= (x_{(11-1 \mod 12)+1}, \cdots, X_{((11-1)+4) \mod 12}) \\ &= (x_{11}, x_{12}, x_1, x_2) \end{aligned}$$

The results of the iteration for the OBB blocks in Eq (2.5) are better arranged in a matrix form.

$$X_t = \begin{pmatrix} x_1 & x_2 & x_3 & x_4 & & & & & & & & \\ & x_2 & x_3 & x_4 & x_5 & & & & & & & \\ & & x_3 & x_4 & x_5 & x_6 & & & & & & \\ & & & & x_5 & x_6 & x_7 & x_8 & & & & \\ & & & & & x_6 & x_7 & x_8 & x_9 & & & \\ & & & & & & x_7 & x_8 & x_9 & x_{10} & & \\ & & & & & & & & x_9 & x_{10} & x_{11} & x_{12} \\ & & & & & & & & & x_{10} & x_{11} & x_{12} \\ & & & & & & & & & & x_{11} & x_{12} \end{pmatrix} \begin{matrix} \mathbf{B_1} \\ \mathbf{B_2} \\ \mathbf{B_3} \\ \mathbf{B_5} \\ \mathbf{B_6} \\ \mathbf{B_7} \\ \mathbf{B_9} \\ \mathbf{B_{10}} \\ \mathbf{B_{11}} \end{matrix} \tag{2.6}$$

Since each block must be unique in element composition blocks with the same element composition regarded as one, blocks B_4 and B_8 are discarded for blocks B_5 and B_9, respectively. In general, the CBB has n number of blocks while OBB has $n - \lfloor \frac{n}{\ell} \rfloor$ number of blocks.

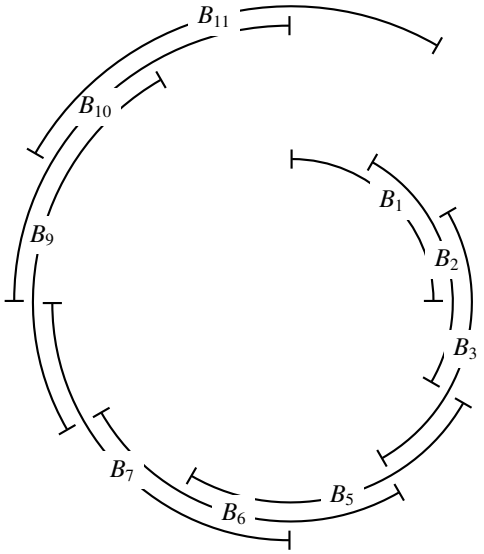

Figure 4. Illustration of OBB.

By comparing Eqs (2.4) and (2.6) also Figures 2 and 4, it is observed that there is reduction in the number of OBB compare to that of CBB from 12 to 9 using the same series data (with $n = 12$ observations) and the same block length ($\ell = 4$). To reduce the number of blocks, the CBB method can be modified by modifying the number of overlaps from m to $m - 1$ in the OBB method. For example, Eq (2.4) in CBB has four overlapping elements in its block arrangement, whereas Eq (2.6) in OBB only has three overlaps. A moderate number of blocks helps to increase the performance of model evaluation metrics (using RMSE and MAE as criteria). In a holistic form, the number of blocks has been reduced from n in CBB to $n - \frac{l}{n}$ in OBB as observed in Eqs (2.2) and (2.5), respectively.

With the CBB and OBB blocks defined to follow the algorithms of Eqs (2.3) and (2.5), respectively, we can now perform the bootstrap. We draw a random sample of blocks with replacements and place them in the bootstrap series in the same order as drawn. Bootstrapped series of blocks for each of the CBB or OBB could be a series of interconnected blocks created or developed like $B_3, B_1, B_5, B_5, B_1, \cdots$ The resampled blocks could be a very large numbering in phantom size represented by R [25].

$$BB = f_{n^*}(x_1^*, x_2^*, \cdots, x_{n^*}^*); \ \left\{ n^* = R \times \ell \right. \tag{2.7}$$

Either the CBB or the OBB bootstrap series is then formed by collapsing elements of B_ι^*; $\iota = 1, 2, \cdots, R$ into a single time series data to form a new time series data, which can be called bootstrap series presented in Eq (2.7).

2.2. Method of data simulation

In this subsection, simulation results to assess the performance of our methodology are presented. The simulated data used in this study exhibits a high degree of versatility, allowing for a thorough evaluation of the bootstrap methods under various conditions. Specifically, the simulation incorporates the following elements:

(1) Varying sample sizes: The analysis covers a range of sample sizes—10, 15, 20, and 25—which allows for an examination of the bootstrap methods' performance across different data volumes. This variation helps assess how well the methods perform when dealing with small to moderate datasets, providing insight into their adaptability.

(2) Here's the rewritten version for clarity and academic tone:

The parameter estimates for the autoregressive model of order one (AR(1)) are given as $\phi = (0.8, 0.9, 0.95)$, while the autoregressive model of order two (AR(2)) is parameterized with $\phi_1 = (0.40, 0.45, 0.35)$ and $\phi_2 = (0.40, 0.45, 0.60)$. Similarly, the moving average model of order one (MA(1)) has parameter estimates of $\theta = (0.8, 0.9, 0.95)$, and the moving average model of order two (MA(2)) is specified with $\theta_1 = (0.40, 0.45, 0.35)$ and $\theta_2 = (0.40, 0.45, 0.60)$. For the autoregressive moving average model of order one-one (ARMA(1,1)), the parameters are $\phi = (0.40, 0.45, 0.35)$ and $\theta = (0.40, 0.45, 0.60)$. These parameter variations facilitate a comprehensive analysis of the model's behavior under differing levels of autocorrelation and moving average effects. Higher values (e.g., 0.95) reflect stronger relationships between current and past values in the time series, allowing for an evaluation of the bootstrap methods' ability to capture these dependencies effectively.

(3) Varying standard deviation: The simulation accounts for different levels of standard deviation (1, 3, 5, and 10), representing varying degrees of noise in the data. This allows the model to be tested under conditions ranging from low to high variability, enabling a comprehensive analysis of how well the bootstrap methods handle noisy versus more stable time series data.

(4) Different orders of ARMA processes: The simulation covers a broad spectrum of ARMA models, including:

   (a) MA(1) and MA(2): These processes capture moving average dynamics of different orders, providing varying levels of smoothing in the time series.

   (b) AR(1) and AR(2): These autoregressive processes model time series with one or two lagged dependencies, offering insight into the performance of bootstrap methods in capturing time series dependencies.

   (c) ARMA(1, 1): This combined autoregressive and moving average model presents more complex dynamics by incorporating both lagged dependencies and smoothing components, testing the bootstrap methods' ability to handle intricate relationships in the data.

Using such diverse simulation settings, this study effectively examines the strengths and weaknesses of the bootstrap methods (CBB and OBB) across a wide range of time series characteristics, ensuring the robustness and versatility of the conclusions drawn from the research.

2.3. Criteria for model and method selection

In order to choose the better-performing method between the two methods (CBB and OBB) discussed above, RMSE is used to choose the best-performing model that results in the better method. Note that [20] deployed RMSE to choose the best-performing method for forecasting the carbon dioxide (CO_2) emission of Bahrain. In evaluating forecasting methods and reporting error statistics,

there has been concern about the most appropriate measure of accuracy. MAE is another metric used in this paper for method evaluation. To evaluate the robustness of data-model comparisons, [13] concluded that RMSE is not enough, rather MAE or other relevant measures are needed. The most common accuracy-fit-performance metric is RMSE.

In [28], RMSE is employed as a primary measure of the error between the predicted and actual RUL values. RMSE is particularly effective at emphasizing larger errors, as it squares the deviations before averaging them. This makes it useful in a context like RUL prediction, where large deviations from the true value can have severe consequences, especially in safety-critical applications like battery management. The study also uses MAE to measure the average magnitude of the prediction errors without considering their direction. Unlike RMSE, which penalizes larger errors more heavily, MAE provides a linear representation of the average absolute error, making it easier to interpret. Overall, [28] demonstrates the effectiveness of RMSE and MAE in evaluating the robustness and accuracy of predictive models. The significant reductions in both metrics illustrate the superiority of the ANA–LSTM model over traditional methods. By incorporating noise handling and adaptive feedback mechanisms, the model achieves enhanced predictive accuracy, which is critical for the safe and efficient operation of lithium-ion battery systems.

Prediction quality is often evaluated by the RMSE or root mean square deviation. Based on Euclidean distance, it shows how far predictions differ from measured true values. To calculate RMSE, calculate the residual (difference between prediction and truth) for each data point, compute its norm, calculate its mean, and then take its square root. As RMSE relies on and requires true measurements at every predicted data point,

$$RMSE = \sqrt{\frac{1}{n}\sum_{\iota=1}^{n}(X_\iota - \hat{X}_\iota)^2} \tag{2.8}$$

$$MAE = \frac{1}{n}\sum_{\iota=1}^{n}|X_\iota - \hat{X}_\iota| \tag{2.9}$$

From the above Eqs (3.1) and (3.2), n is the number of data points, X_ι is the i-th measurement, and $\hat{X}_t$ is its corresponding prediction. MAE also has the same units as RMSE [4]. Usually, MAE is smaller than RMSE, although it can be the opposite if the predicted values are very close to the observed.

One keepS varying the block length to test for the minimum RMSE and MAE [8]. We are interested in the same statistic for both CBB and OBB (the estimates of ARIMA parameters), and here is what we generally expect when we resample blocks from each algorithms' phantom times:

(1) **Estimates of the mean (or other statistics):**

   (a) You would obtain an empirical bootstrap distribution of the ARIMA parameters for both CBB and OBB methods.

   (b) The central limit theorem suggests that these distributions of the ARIMA parameters should be approximately normally distributed, even more so with a large number of resamples.

(2) **Variability:**

   (a) The CBB method, with more distinct elements, might show greater variability in its bootstrap distribution if the underlying population distribution is also more variable.

(b) The OBB, with fewer distinct elements, might show less variability, assuming the original nine elements are less variable.

(3) **Confidence intervals:**

(a) One could calculate confidence intervals for the ARIMA parameters (or other parameters) from the bootstrap distributions.

(b) The wider range of elements in the CBB might lead to a wider confidence interval, due to more variability, compared to the OBB method.

(4) **Bias and accuracy:**

(a) Both CBB and OBB would allow for an estimate of the bias and standard error of the statistic of interest.

(b) The accuracy of these estimates would improve with the number of bootstrap samples (i.e., resampling many times reduces the error in the estimate).

In summary, when comparing the bootstrap estimates from CBB and OBB, you would likely find differences in the variability of the estimates due to the difference in the number of distinct elements. The sample with more unique values (CBB) will likely show a wider spread in the bootstrap distribution, assuming underlying population distributions are consistent with the sample representations [9]. This scenario is based on the assumption that other conditions are equal, such as the distribution from which the samples were taken. It's also important to remember that the bootstrap method provides empirical estimates and the actual results can be influenced by the specific characteristics of the original samples.

Listing 1. OBL Package for Minimum RMSE Values

```
> require(OBL)
> df <- OBL::blockboot(ts, 1000, n_cores = 1, seed = 6)
> df$RMSE[2]
# [1] 0.3286192
```

Listing 2. OBL Package for Minimum MAE Values

```
> require(OBL)
> df <- OBL::blockboot(ts, 1000, n_cores = 1, seed = 6)
> df$RMSE[3]
# [1] 0.3398036
```

This proposed method can be executed with the help of an R package in [5] using R programming language in [26] as demonstrated in Listing 1 to obtain each value of RMSE; MAE can be obtained using a similar command in the same R package [5] as demonstrated in Listing 2. The R code demonstrated in Listings 1 and 2 is applicable to both simulated and real life data.

2.4. Summary of methodology comparison of CBB and OBB

In order to justify the efficiency of the newly proposed block bootstrap method (OBB) compared to the conventional block bootstrap method (CBB), here's a mathematical methodology:

(1) **Block bootstrap definitions**:

(a) **Block formation for CBB and OBB**:

(i) **CBB**: Each block is defined as $B_\iota = x_\iota, \cdots, x_{\iota+\ell-1}$ where $1 < \ell < n$ is a positive integer.

(ii) **OBB**: Each block is defined as $B_\iota = x_{\iota+0 \bmod (\iota,\ell)}, \cdots, x_{\iota+0 \bmod (\iota,\ell)+\ell-1}$.

(b) **Overlapping size**:

(i) **CBB** method divides the time series into blocks of equal length ℓ with overlapping parameter $M_{CBB} = \ell$.

(ii) **OBB** method divides the time series into blocks of equal length ℓ with overlapping parameter $M_{OBB} = \ell - 1$.

(c) **Number of block**:

(i) **CBB**: The CBB method divides the time series into blocks of equal length ℓ, where the number of blocks is n, i.e., $B_i = B_1, B_2, \cdots, B_n$.

(ii) **OBB**: The newly proposed OBB method divides the given time series data into blocks of length ℓ as well, but with the number of blocks being $n-\lfloor n/\ell \rfloor$ ie $B_\iota = B_1, B_2, \cdots, B_{n-\lfloor n/\ell \rfloor}$.

(d) **Number of resample**:

(i) CBB method selects R resamples from $B_\iota; \iota = 1, 2, \cdots, n$ where R ¿ n.

(ii) OBB method selects R resamples from $B_\iota; \iota = 1, 2, \cdots, (n - \lfloor n/\ell \rfloor)$.

(2) **Mathematical justification**:

(a) **Resampling blocks**:

(i) In CBB, R resamples are drawn from n blocks.

(ii) In OBB, R resamples are drawn from $n - |n/l|$ blocks.

(3) **Efficiency comparison**:

(a) **Efficiency measure**: Efficiency here refers to the quality of the resampling method in preserving statistical properties. A more efficient method will yield estimates closer to the true values with fewer samples.

(b) **Comparison point**: Compare the statistical efficiency of CBB and OBB through their respective resampling procedures.

(4) **Consideration of exemption from resampling**:

(a) **CBB method**: Since there are more number of blocks (n) compared to $n - |n/l|$ blocks in OBB, there is a higher chance that a block will be exempted from being resampled compared with OBB.

(b) **OBB method**: In another way, since there are fewer blocks $(n - |n/l|)$ compared to n blocks in CBB, there is less chance that a block will be exempted from being resampled.

(5) **Conclusion**:

(a) From the above comparison, despite both methods utilizing blocks of length ℓ, OBB's reduced number of blocks $n - |n/l|$ implies a higher chance of each block being included in the resampling process compared to CBB's n blocks. This higher inclusivity in OBB greatly contribute to better overall efficiency by retaining more information from the original series.

2.5. Algorithm for determination of optimal number blocks

The efficient block bootstrap method determination for forecasting with ARIMA models is obtained as follows:

(1) Given a time series data such as demonstrated in Eq (2.1), which follows a form or subset of ARIMA models as described in Eq (2.2), determine the order of the $ARIMA(p, d, q)$.
(2) Arbitrarily choose some block sizes ℓ from $1 < \ell < n$.
(3) Form the bootstrap blocks by churning an ARIMA time series into smaller "subseries" as described in Eqs (2.3) and (2.6) for the CBB and OBB methods, respectively.
(4) Resample a set of "R-samples" with replacement from $\{B_\iota\} = \{B_1, B_2, \cdots, B_n\}$ and $\{B_\iota\} = \{B_1, B_2, \cdots, B_{n-\lfloor n/l \rfloor}\}$ for the CBB and OBB methods, respectively, such that $(n < R < \infty)$, to be called bootstrap samples.
(5) Compute RMSE and MAE each for the CBB and OBB block described in item 2.5.
(6) Sequentially repeat step 2.5 to 2.5 z-times $(n < z < \infty)$ to get an average of $RMSE$ as $\frac{1}{z}\sum_{\iota=1}^{z}(\sqrt{MSE})$ and MAE as $\frac{1}{m}\sum_{\iota=1}^{z}(MAE)$ for the CBB and OBB methods described in Eqs (2.3) and (2.6), respectively, using Monte-Carlo's method.

3. Results

This section presents an in-depth analysis of the performance of two bootstrap methods, the CBB and OBB, applied to both simulated and real-life time series data. To evaluate the accuracy of these methods, two key error metrics—RMSE and MAE—were employed. RMSE was used to emphasize larger deviations in prediction, while MAE provided a straightforward measure of average error magnitude. The comparative analysis across various datasets, including different sample sizes and parameter configurations, enables a comprehensive understanding of how each method performs in terms of accuracy and robustness. The findings reveal notable differences between the two methods, offering valuable insights into their respective strengths and weaknesses in time series forecasting.

3.1. Simulated study

This subsection presents a comparative analysis where different ARMA time series processes are simulated and analyzed using the CBB and OBB methods and the values of their RMSE and MAE are arranged.The various time series models including autoregressive of order one (AR(1)) process, autoregressive of order two (AR(2)) process, moving average of order one (MA(1)) process, moving average of order two (MA(2)) process, autoregressive of order one with moving average of order of order one (ARMA(1,1)) process, autoregressive of order two with moving average of order of order one (ARMA(2,1)) process, and autoregressive of order one with moving average of order of order two (ARMA(1,2)) process. The RMSE values of the two methods are displayed side-by-side in tables while the values of the MAE are displayed in grid-plots, allowing for a systematic evaluation of the methods' predictive performance under different sample sizes, autoregressive and moving average parameters, and standard deviations.

Table 1 provides a detailed comparison of the RMSE values for the two bootstrap methods, CBB and OBB, across 12 AR(1) processes under different conditions. The table is structured with sample

sizes (10, 15, 20, 25) in the minor columns, while the major columns display the estimated AR(1) parameters, ϕ (0.80, 0.90, 0.95), and standard deviation levels (1, 3, 5, 10) in the major rows. The results reveal that OBB consistently produces smaller RMSE values compared to CBB, indicating better prediction accuracy. Figure 5 complements these findings by illustrating the corresponding MAE values for both methods. The facet-grid plot displays ϕ values along the major columns and standard deviation levels across the rows, with sample sizes represented on the x-axis. Solid lines connect the MAE values for CBB, while dotted lines represent OBB, offering a clear visual comparison of the methods' performance under varying conditions.

Table 2 offers a comparative analysis of the RMSE values for the CBB and OBB methods applied to 12 AR(2) processes under varying conditions, structured similarly to the AR(1) process. The minor columns present sample sizes (10, 15, 20, 25), while the major columns display the estimated AR(2) parameters, ϕ_1 (0.40, 0.45, 0.35) and ϕ_2 (0.40, 0.45, 0.60). The results are further categorized by standard deviation levels (1, 3, 5, 10) in the major rows, consistently showing that OBB outperforms CBB with lower RMSE values across all conditions. Figure 6 complements this analysis by visualizing the MAE values for both methods using facet-grid plot. Each dot represents the MAE for CBB and OBB, connected by solid and dotted lines, respectively. The facet grid presents the AR(2) parameter estimates along the major columns and standard deviation levels across the rows, with the x-axis showing sample sizes, facilitating a clear comparison of the methods' MAE performance under different conditions.

Table 3 presents the RMSE values for the CBB and OBB methods applied to 12 MA(1) processes under varying conditions. The structure follows that of the AR models, with sample sizes (10, 15, 20, 25) in the minor columns and the MA(1) parameter estimates, θ (0.80, 0.90, 0.95), in the major columns. Different standard deviation levels (1, 3, 5, 10) are displayed in the major rows. The OBB method consistently yields smaller RMSE values than CBB, indicating superior predictive performance. Figure 7 complements this by illustrating the MAE values for the same MA(1) processes and bootstrap methods. Dots represent the MAE values, with solid lines connecting the CBB values and dotted lines for the OBB values. The facet grid displays θ (0.80, 0.90, 0.95) along the major columns, and standard deviation levels (1, 3, 5, 10) across the rows. The x-axis in each cell represents sample sizes, enabling a detailed comparison of MAE performance under different conditions.

Table 4 compares the RMSE values for the CBB and OBB methods applied to 12 MA(2) processes, with sample sizes (10, 15, 20, 25) in the minor columns and MA(2) parameter estimates, θ_1 (0.40, 0.45, 0.35) and θ_2 (0.40, 0.45, 0.60), in the major columns. Results are further stratified by standard deviations (1, 3, 5, 10). The OBB method consistently outperforms CBB by yielding lower RMSE values across all conditions, demonstrating better prediction accuracy. Figure 8 complements the table by illustrating the MAE values for the same MA(2) processes. Dots represent MAE values for both methods, with solid lines connecting the CBB values and dotted lines connecting the OBB values. The facet-grid plot arranges θ_1 and θ_2 estimates along the major columns, while different standard deviation levels (1, 3, 5, 10) appear across the rows. Each cell's x-axis shows the sample sizes, facilitating a detailed comparison of MAE performance across varying conditions.

Table 1. Minimum RMSE criterion of CBB and OBB methods for AR(1).

	$\varphi = 0.8$				$\varphi = 0.9$				$\varphi = 0.95$				
n	**10**	**15**	**20**	**25**	**10**	**15**	**20**	**25**	**10**	**15**	**20**	**25**	
CBB	0.59	0.97	1.72	1.97	0.96	1.45	1.79	1.50	1.43	1.29	1.50	1.22	***sd* = 1**
OBB	0.57	0.96	1.68	1.94	0.95	0.46	1.72	1.49	1.41	1.23	1.44	1.17	
CBB	4.76	2.91	5.17	5.91	2.88	4.38	5.38	4.50	4.30	3.86	4.51	3.66	***sd* = 3**
OBB	4.75	2.88	5.05	5.81	2.84	4.35	5.17	4.46	4.24	3.69	4.32	3.51	
CBB	7.93	4.85	8.61	9.85	4.80	7.30	8.96	7.50	7.17	6.43	7.51	6.09	***sd* = 5**
OBB	7.91	4.80	8.41	9.69	4.73	7.24	8.62	7.43	7.07	6.15	7.21	5.85	
CBB	15.86	9.70	17.23	19.71	9.60	14.61	17.93	15.00	14.35	12.86	15.03	12.18	***sd* = 10**
OBB	15.82	9.61	16.83	19.38	9.46	14.49	17.24	14.87	14.14	12.30	14.42	11.69	

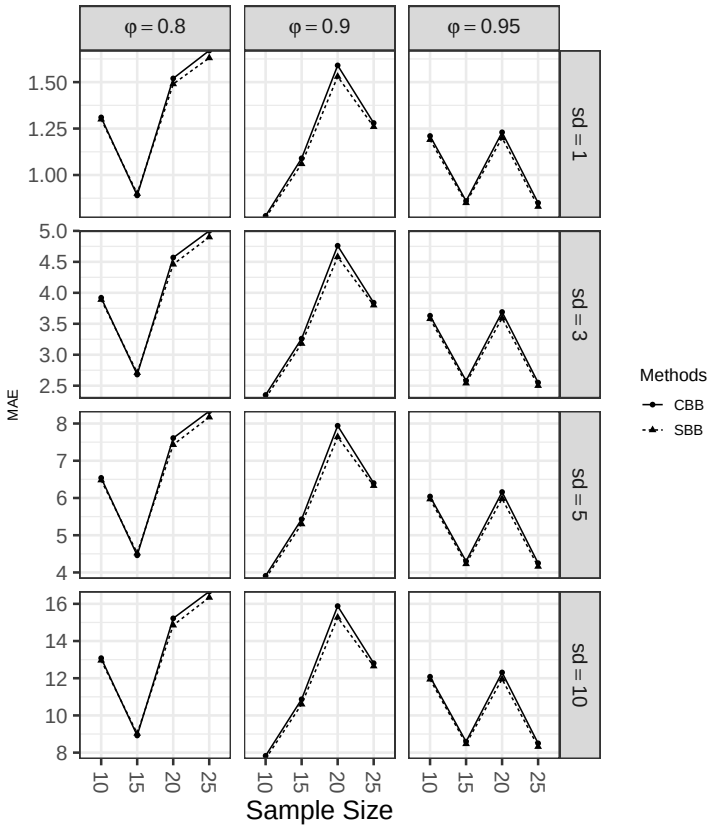

Figure 5. Facet-Grid plot of minimum MAE of CBB and OBB methods for AR(1).

Table 2. Minimum RMSE criterion of CBB and OBB methods for AR(2).

	$\varphi_1 = 0.4,\ \varphi_2 = 0.4$				$\varphi_1 = 0.45,\ \varphi_2 = 0.45$				$\varphi_1 = 0.35,\ \varphi_2 = 0.6$				
n	**10**	**15**	**20**	**25**	**10**	**15**	**20**	**25**	**10**	**15**	**20**	**25**	
CBB	0.80	1.42	1.17	1.44	1.19	1.19	1.72	1.28	1.21	1.13	1.53	1.42	***sd* = 1**
OBB	0.74	1.41	1.16	1.42	1.05	1.17	1.71	1.27	1.18	1.11	1.47	1.41	
CBB	2.41	4.25	3.50	4.33	3.57	3.58	4.53	3.83	3.62	3.40	4.60	4.27	***sd* = 3**
OBB	2.21	4.24	3.47	4.25	3.16	3.52	4.50	3.81	3.54	3.33	4.41	4.22	
CBB	4.02	7.08	5.84	7.22	5.94	5.96	7.54	6.38	6.03	5.66	7.67	7.11	***sd* = 5**
OBB	3.69	7.07	5.78	7.09	5.27	5.87	7.50	6.36	5.90	5.56	7.35	7.03	
CBB	8.04	14.16	11.67	14.45	11.89	11.93	15.09	12.76	12.07	11.33	15.33	14.23	***sd* = 10**
OBB	7.38	14.13	11.57	14.17	10.54	11.75	15.00	12.72	11.80	11.11	14.70	14.05	

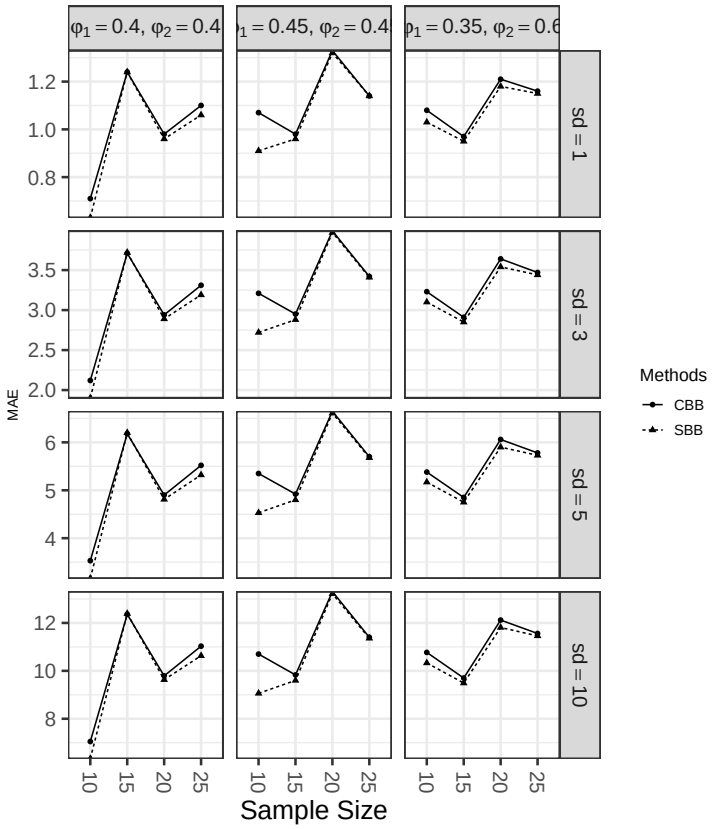

Figure 6. Facet-Grid plot of minimum MAE of CBB and OBB methods for AR(2).

Table 3. Minimum RMSE criterion of CBB and OBB methods for MA(1).

	$\vartheta = 0.8$				$\vartheta = 0.9$				$\vartheta = 0.95$				
n	**10**	**15**	**20**	**25**	**10**	**15**	**20**	**25**	**10**	**15**	**20**	**25**	
CBB	0.87	1.11	1.34	1.71	1.34	1.08	1.26	1.25	1.44	1.33	1.09	1.32	***sd* = 1**
OBB	0.85	1.08	1.31	1.60	1.32	1.07	1.19	1.17	1.41	1.24	1.05	1.31	
CBB	2.61	3.32	4.01	5.12	4.01	3.25	3.77	3.75	4.31	3.98	3.28	3.95	***sd* = 3**
OBB	2.56	3.23	3.94	4.79	3.95	3.21	3.57	3.52	4.22	3.72	3.14	3.93	
CBB	4.35	5.53	6.69	8.53	6.69	5.42	6.28	6.25	7.18	6.63	5.47	6.58	***sd* = 5**
OBB	4.27	5.38	6.57	7.99	6.59	5.35	5.95	5.86	7.04	6.20	5.23	6.54	
CBB	8.69	11.05	13.38	17.06	13.38	10.83	12.55	12.49	14.36	13.26	10.95	13.17	***sd* = 10**
OBB	8.55	10.77	13.14	15.98	13.18	10.70	11.91	11.72	14.07	12.40	10.45	13.08	

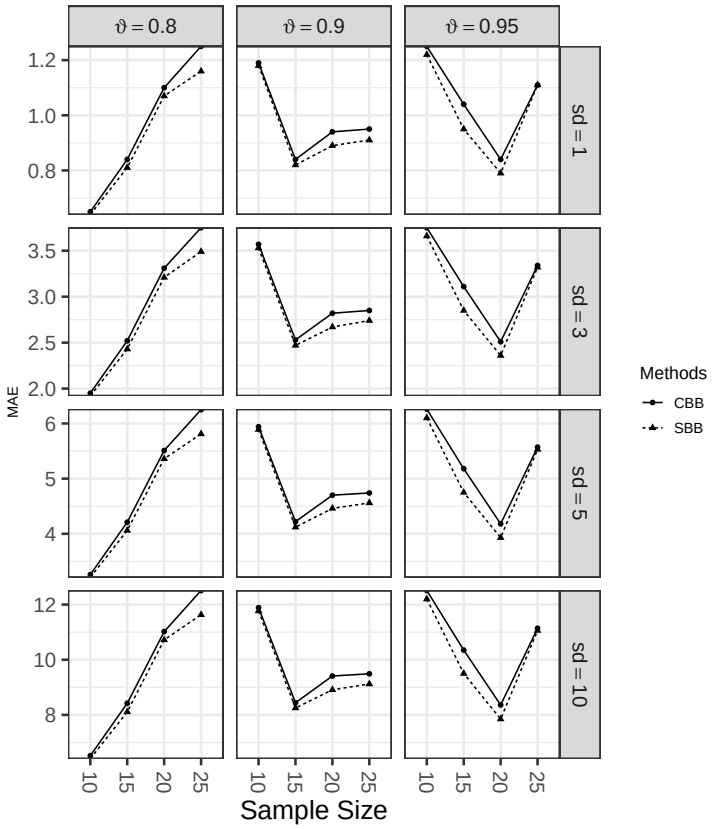

Figure 7. Facet-Grid plot of minimum MAE of CBB and OBB methods for MA(1).

Table 4. Minimum RMSE criterion of CBB and OBB methods for MA(2).

	$\vartheta_1 = 0.4, \vartheta_2 = 0.4$				$\vartheta_1 = 0.45, \vartheta_2 = 0.45$				$\vartheta_1 = 0.35, \vartheta_2 = 0.6$				
n	**10**	**15**	**20**	**25**	**10**	**15**	**20**	**25**	**10**	**15**	**20**	**25**	
CBB	0.87	1.31	1.25	1.32	5.12	1.25	1.47	1.36	1.17	1.32	1.15	1.25	***sd* = 1**
OBB	0.85	1.29	1.23	1.28	1.76	1.22	1.41	1.32	1.13	1.26	1.15	1.24	
CBB	2.61	3.93	3.76	3.96	5.28	3.76	4.41	4.09	3.52	3.97	3.46	3.76	***sd* = 3**
OBB	2.56	3.87	3.68	3.85	5.12	3.65	4.24	3.96	3.38	3.79	3.43	3.73	
CBB	4.35	6.54	6.27	6.60	8.80	6.27	7.35	6.82	5.87	6.62	5.76	6.27	***sd* = 5**
OBB	4.27	6.45	6.13	6.42	8.53	6.09	7.07	6.59	5.63	6.31	5.72	6.22	
CBB	8.71	13.09	12.54	13.19	17.61	12.55	14.69	13.63	11.75	13.23	11.52	12.55	***sd* = 10**
OBB	8.53	12.91	12.26	12.83	17.07	12.18	14.15	13.19	11.26	12.63	11.45	12.44	

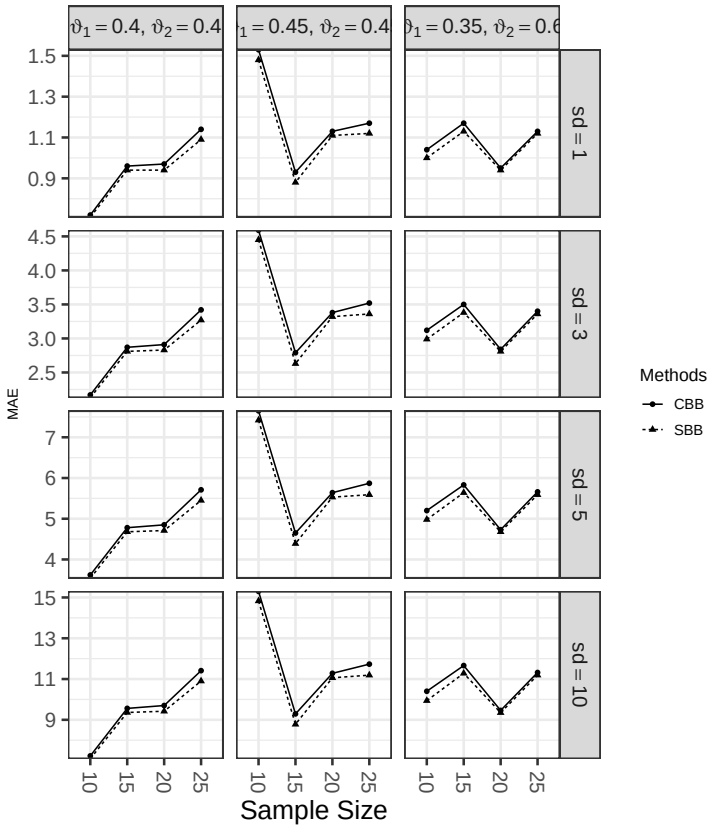

Figure 8. Facet-Grid plot of minimum MAE of CBB and OBB methods for MA(2).

Table 5. Minimum RMSE criterion of CBB and OBB methods for ARMA(1, 1).

	$\varphi_1 = 0.5,\ \vartheta_2 = 0.3$				$\varphi_1 = 0.5,\ \vartheta_2 = 0.4$				$\varphi_1 = 0.35,\ \vartheta_2 = 0.6$				
n	**10**	**15**	**20**	**25**	**10**	**15**	**20**	**25**	**10**	**15**	**20**	**25**	
CBB	1.22	1.11	1.47	1.35	1.22	1.66	1.92	1.13	1.20	1.17	1.43	1.32	***sd* = 1**
OBB	1.18	1.06	1.44	1.34	1.19	1.64	1.91	1.09	1.18	1.16	1.42	1.30	
CBB	3.66	3.33	4.41	4.05	3.67	4.98	5.76	3.38	3.61	3.50	4.29	3.96	***sd* = 3**
OBB	3.54	3.18	4.31	4.01	3.58	4.92	5.74	3.27	3.53	3.47	4.27	3.90	
CBB	6.10	5.56	7.35	6.75	6.12	8.31	9.60	5.63	6.01	5.83	7.15	6.60	***sd* = 5**
OBB	5.90	5.30	7.18	6.68	5.97	8.20	9.56	5.45	5.88	5.78	7.11	6.49	
CBB	12.20	11.11	14.70	13.49	12.24	16.61	19.20	11.25	12.02	11.67	14.30	13.21	***sd* = 10**
OBB	11.81	10.59	14.37	13.35	11.94	16.40	19.13	10.90	11.77	11.55	14.23	12.98	

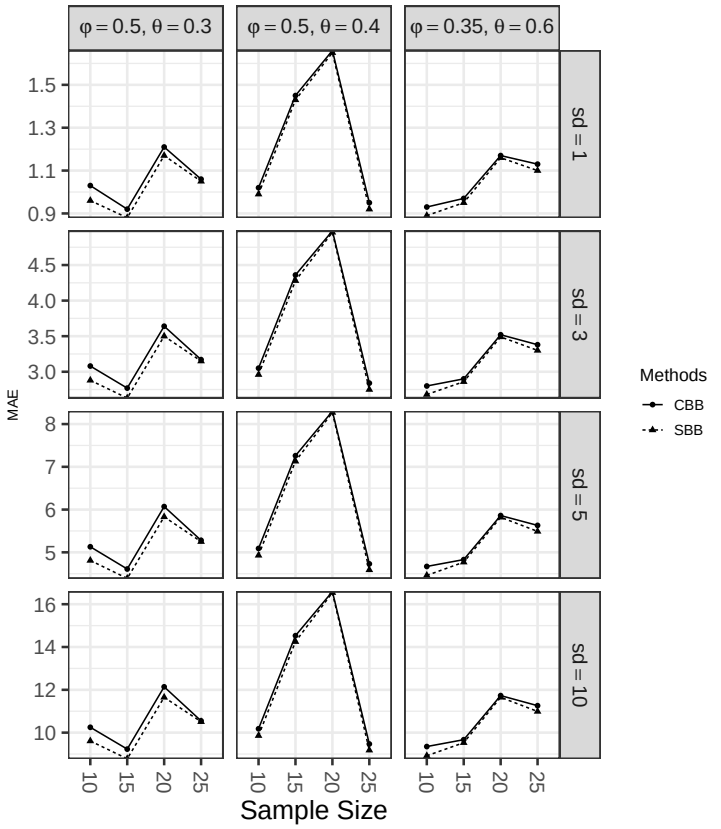

Figure 9. Facet-Grid plot of minimum MAE of CBB and OBB methods for ARMA(1, 1).

Table 6. Minimum RMSE criterion of CBB and OBB methods for ARMA(2, 1).

	$\varphi_1 = 0.5,\ \varphi_2 = 0.1,\ \vartheta = 0.2$				$\varphi_1 = 0.6,\ \varphi_2 = 0.2,\ \vartheta = 0.1$				$\varphi_1 = 0.5,\ \varphi_2 = 0.3,\ \vartheta = 0.15$				
n	**10**	**15**	**20**	**25**	**10**	**15**	**20**	**25**	**10**	**15**	**20**	**25**	
CBB	1.65	1.63	1.00	0.99	1.51	1.36	1.85	0.97	1.01	1.03	1.46	1.54	***sd* = 1**
OBB	1.60	1.55	0.98	0.98	1.32	0.92	1.76	1.10	1.18	1.02	1.45	1.52	
CBB	4.75	4.89	2.86	3.27	4.55	4.07	6.77	2.88	3.66	3.42	5.09	4.77	***sd* = 3**
OBB	3.95	4.80	2.38	2.92	3.98	4.58	6.69	2.81	3.52	3.29	5.34	4.94	
CBB	6.79	8.16	4.93	4.93	6.82	6.94	10.70	4.79	5.18	5.33	8.07	7.32	***sd* = 5**
OBB	6.53	7.78	4.90	4.89	6.65	7.07	10.62	4.73	5.52	5.33	8.60	7.63	
CBB	16.27	16.25	9.97	9.84	13.57	14.78	17.49	9.74	10.04	10.54	18.34	17.35	***sd* = 10**
OBB	11.87	15.53	10.82	12.11	11.92	13.45	17.39	10.60	11.12	10.98	18.28	17.20	

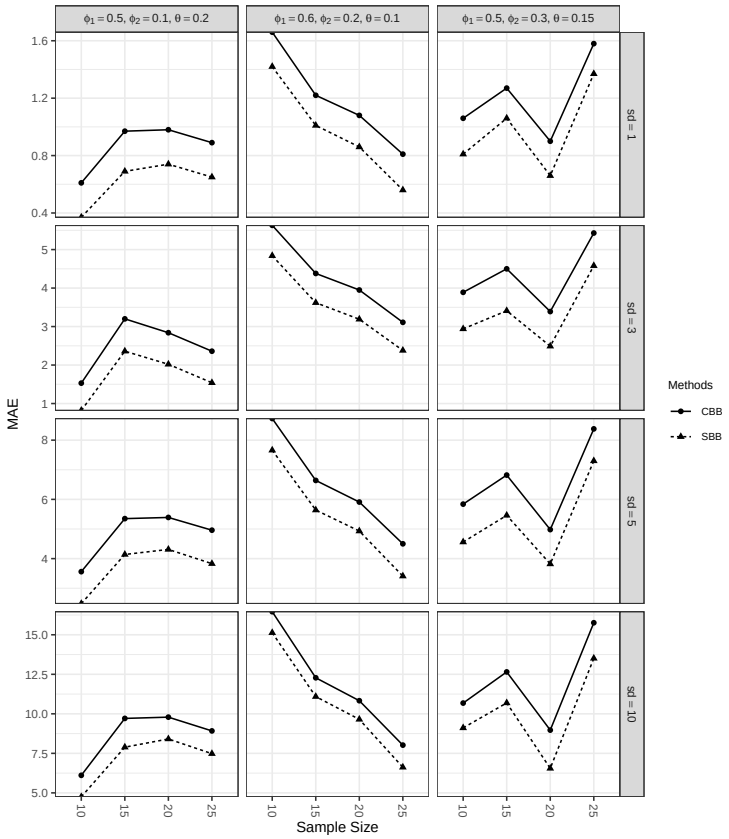

Figure 10. Facet-Grid plot of minimum MAE of CBB and OBB methods for ARMA(2, 1).

Table 7. Minimum RMSE criterion of CBB and OBB methods for ARMA(1, 2).

	$\varphi = 0.4,\ \vartheta_1 = 0.2,\ \vartheta_2 = 0.2$				$\varphi = 0.5,\ \vartheta_1 = 0.25,\ \vartheta_2 = 0.15$				$\varphi = 0.6,\ \vartheta_1 = 0.2,\ \vartheta_2 = 0.15$				
n	**10**	**15**	**20**	**25**	**10**	**15**	**20**	**25**	**10**	**15**	**20**	**25**	
CBB	2.43	2.20	0.73	0.66	8.06	1.17	1.52	0.88	0.83	1.06	1.12	1.58	***sd* = 1**
OBB	2.36	2.09	0.71	0.66	6.60	0.79	1.44	0.99	0.97	1.04	1.16	1.56	
CBB	7.08	6.60	2.08	2.19	8.34	3.50	4.90	1.93	2.87	3.42	3.89	4.96	***sd* = 3**
OBB	5.78	6.44	1.73	1.96	7.29	3.94	4.83	1.87	2.77	3.19	4.15	5.04	
CBB	9.91	10.97	3.59	3.27	12.30	5.79	8.91	4.26	4.24	5.48	6.16	7.35	***sd* = 5**
OBB	9.53	10.44	3.56	3.25	12.01	5.92	8.88	4.20	4.41	5.48	6.53	7.84	
CBB	29.44	21.91	7.27	6.60	24.57	12.31	14.87	7.19	8.03	13.13	13.91	23.02	***sd* = 10**
OBB	17.39	20.82	7.88	8.07	21.58	11.20	15.29	8.03	8.79	13.61	13.90	22.89	

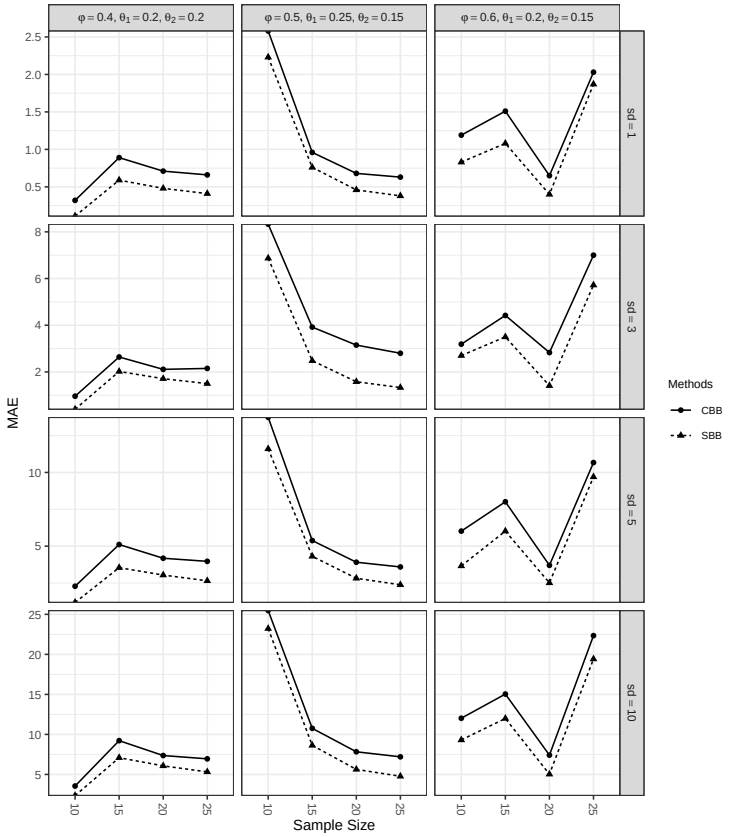

Figure 11. Facet-Grid plot of minimum MAE of CBB and OBB methods for ARMA(1, 2).

Table 5 compares the RMSE values for the CBB and OBB methods applied to 12 ARMA(1,1)

processes, with sample sizes (10, 15, 20, 25) in the minor columns. The first combination comprises $\phi = 0.50$, $\theta = 0.30$; the second combination includes $\phi = 0.50$, $\theta = 0.40$; and the third combination consists of $\phi = 0.35$, $\theta = 0.60$. The data is further categorized by different standard deviation levels (1, 3, 5, 10). The OBB method consistently achieves lower RMSE values across all conditions, highlighting its superior predictive accuracy. Figure 9 complements this table by illustrating the MAE values for the ARMA(1,1) process in a facet-grid plot, with dots representing MAE values for CBB and OBB, connected by solid and dotted lines, respectively. The facet grid arranges the parameter estimates ϕ and θ along the major columns, with varying standard deviations across the rows. Each cell's x-axis corresponds to the sample sizes, providing a detailed comparison of MAE performance under different conditions.

Table 6 presents a comparison of RMSE values for the CBB and OBB methods applied to 12 ARMA(2,1) processes. The minor columns display sample sizes (10, 15, 20, 25), while the major columns represent different combinations of ARMA(2,1) parameter estimates. The first combination comprises $\phi_1 = 0.50$, $\phi_2 = 0.10$, and $\theta = 0.20$; the second combination includes $\phi_1 = 0.60$, $\phi_2 = 0.20$, and $\theta = 0.10$; and the third combination consists of $\phi_1 = 0.50$, $\phi_2 = 0.30$, and $\theta = 0.15$. The data is further categorized by standard deviation levels (1, 3, 5, 10). The OBB method consistently produces lower RMSE values across all conditions, demonstrating its superior predictive accuracy. Figure 10 complements this table by displaying the MAE values for the ARMA(2, 1) process in a facet-grid plot. Dots represent MAE values for both CBB and OBB methods, connected by solid and dotted lines, respectively. The facet grid arranges the parameter estimates ϕ_1, ϕ_2, and θ in the major columns, with varying standard deviations across the rows. The x-axis in each cell corresponds to the sample sizes, offering a detailed comparison of MAE performance under different conditions.

Table 7 presents a comparison of RMSE values for the CBB and OBB methods applied to 12 ARMA(2,1) processes. The minor columns display sample sizes (10, 15, 20, 25), while the major columns represent different combinations of ARMA(2,1) parameter estimates. The first combination comprises $\phi = 0.40$, $\theta_1 = 0.20$, and $\theta_2 = 0.20$; the second combination includes $\phi = 0.50$, $\theta_1 = 0.25$, and $\theta_2 = 0.15$; and the third combination consists of $\phi = 0.60$, $\theta_1 = 0.20$, and $\theta_2 = 0.15$. The data is further categorized by standard deviation levels (1, 3, 5, 10). The OBB method consistently produces lower RMSE values across all conditions, demonstrating its superior predictive accuracy. Figure 11 complements this table by displaying the MAE values for the ARMA(1, 2) process in a facet-grid plot. Dots represent MAE values for both CBB and OBB methods, connected by solid and dotted lines, respectively. The facet grid arranges the parameter estimates ϕ_1, ϕ_2, and θ in the major columns, with varying standard deviations across the rows. The x-axis in each cell corresponds to the sample sizes, offering a detailed comparison of MAE performance under different conditions.

In summary, across all models and varying conditions, the OBB method consistently produces smaller RMSE and MAE values compared to CBB, highlighting its robustness and improved performance in time series prediction. The comparison across AR(1), AR(2), MA(1), MA(2), ARMA(1, 1), ARMA(2, 1), and ARMA(1, 2) processes demonstrates that the OBB method offers a clear advantage in terms of prediction accuracy. The prediction quality of the OBB method is consequently shown to be better than the existing method CBB method.

3.2. *Real life data applications*

Four South African's economic data were collected chronologically on an annual basis, namely: the inflation rate, the GDP growth rate, the interest rate and the unemployment rate. The data is adopted from the Macrotrend web page [16] on https://www.macrotrends.net/countries/ZAF/south-africa/gdp-growth-rate. Data on inflation rate ranges from 1971 to 2022, data on GDP growth rate ranges from 1964 to 2022, data on interest rate ranges from 1980 to 2022, while that of unemployment rate ranges from 1995 to 2022. In order to get a better view of the data, time plots of the economic data are presented in Figures 12–15 below.

Based on the visual representation of each time series in Figures 12–15, the block bootstrap procedure was applied to the time series data using both the CBB and OBB methods. The objective was to determine the optimal block length and to calculate the resulting RMSE values for each method. Table 8 summarizes the optimal block lengths obtained for each method (CBB and OBB) across the four time series: inflation rate, GDP growth rate, interest rate, and unemployment rate. The methodologies employed for these calculations are described in Subsection 2.5, and implemented using an R package developed by [5], which is documented and accessible at https://cran.r-project.org/web/packages/OBL/vignettes/OBL.html.

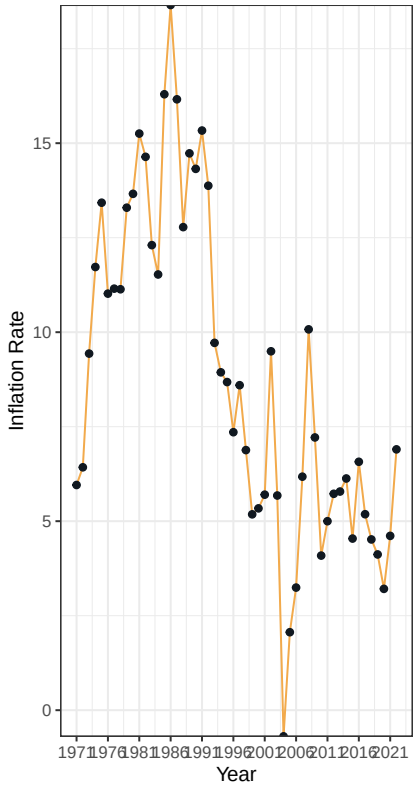

Figure 12. Time series plot of the inflation data.

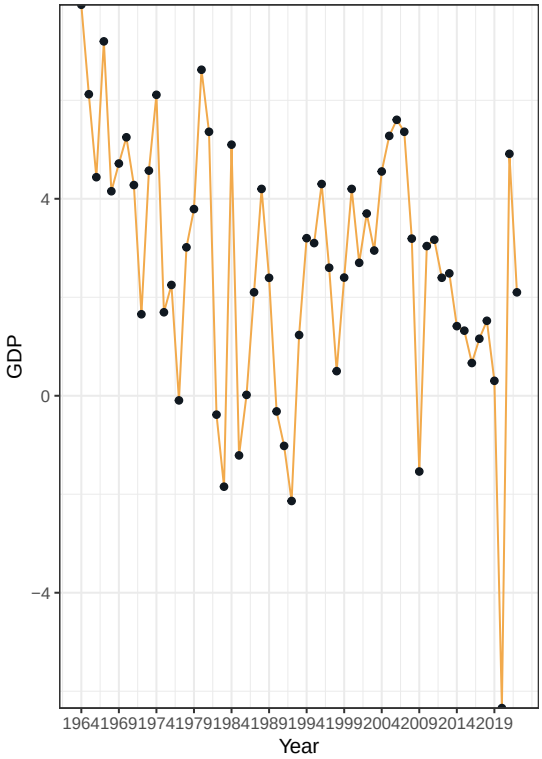

Figure 13. Time series plot of the GDP growth rate (in percentage).

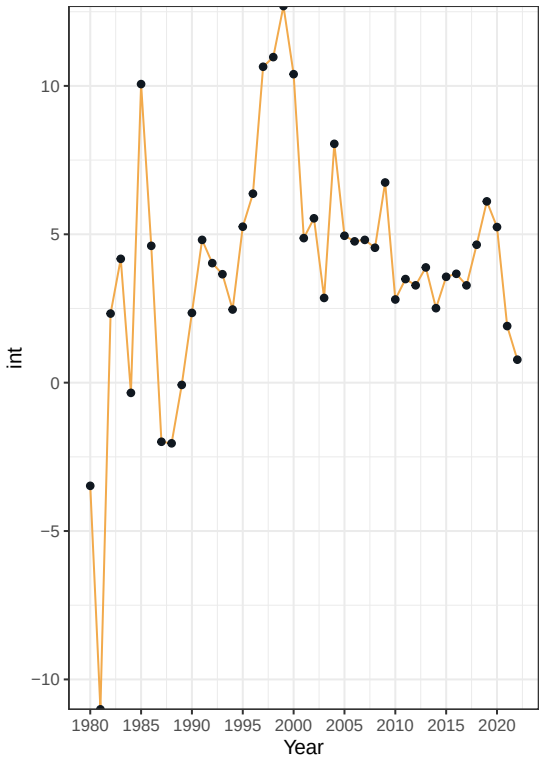

Figure 14. Time series plot of the interest rate data.

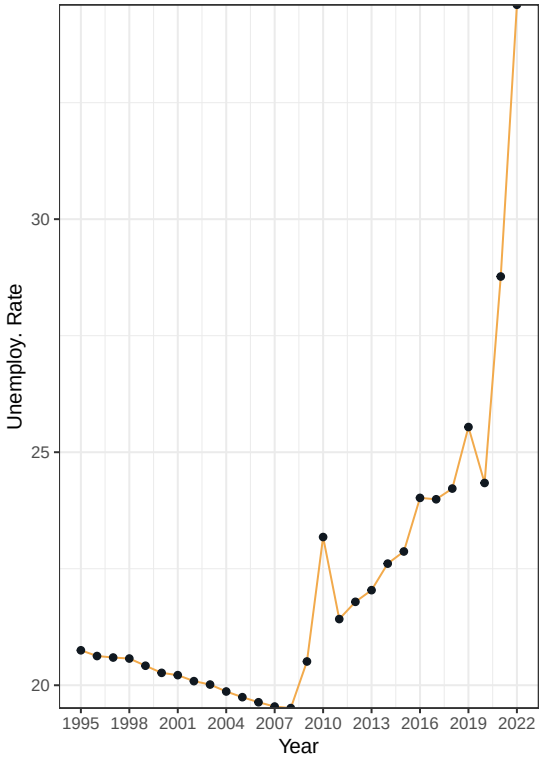

Figure 15. Time series plot of the unemployment rate data.

For illustration, inflation rate data is split to block length of 27 before bootstrap for the CBB method while the same data is split block length of 34 before block resample for the OBB method. Every other economic data was bootstrapped according to a similar procedure as presented in Table 8.

Table 8. Accuracy-metric table for model obtained from CBB and OBB methods.

Variable	Sample Size	Method	Optimal Block Length	RMSE	MAE
Inflation Rate	52	CBB	27	3.817	2.255
		OBB	34	2.438	1.794
GDP	58	CBB	34	2.586	1.794
		OBB	34	2.231	1.751
Interest Rate	42	CBB	11	2.900	2.039
		OBB	40	2.792	1.770
Unemployment Rate	24	CBB	16	5.418	2.610
		OBB	26	1.768	1.123

An investigation is made to check for model performance for the ARIMA model obtained through the CBB method and the ARIMA model obtained through the OBB method for each time series data. Each pair of metric comparison on Table 8 shows that the ARIMA models selected through the OBB method perform better than that the ones selected through the CBB method for each time series data. The model comparison table presented in Table 8 shows that the RMSE value of the model selected through the OBB method is smaller than the corresponding RMSE value of the model selected through

the CBB method. The case of RMSE is the same for MAE values for every time series data presented. It is also observed that the value of MAE for each method and for every time series data is less than its RMSE counterpart.

$$\begin{aligned}\hat{X}_t =& 8.1541 + 0.3329X_{t-1} - 0.1345X_{t-2} - 0.1678X_{t-3} - 0.0167X_{t-4} + \\ & 0.6771X_{t-5} + 0.7468\varepsilon_{t-1} + 0.4829\varepsilon_{t-2} + 0.8139\varepsilon_{t-3} + \\ & 0.7578\varepsilon_{t-4} - 0.2443\varepsilon_{t-5} + \varepsilon_t\end{aligned} \tag{3.1}$$

$$\begin{aligned}\hat{X}_t =& 4.0874 + 1.0967X_{t-1} - 0.9659X_{t-2} + 0.0694X_{t-3} + 0.0068X_{t-4} - \\ & 0.3457X_{t-5} - 1.0452\varepsilon_{t-1} + 0.7150\varepsilon_{t-2} + \varepsilon_t\end{aligned} \tag{3.2}$$

$$\begin{aligned}\hat{X}_t =& 6.8857 + 2.0485X_{t-1} - 1.7055X_{t-2} + 0.4035X_{t-3} + 0.2293X_{t-4} - \\ & 0.2284X_{t-5} - 1.5314\varepsilon_{t-1} - 0.8628\varepsilon_{t-2} + \varepsilon_t\end{aligned} \tag{3.3}$$

$$\begin{aligned}\hat{X}_t =& 21.5468 + 1.8219X_{t-1} - 0.9727X_{t-2} - 1.3439\varepsilon_{t-1} + 0.2202\varepsilon_{t-2} + \\ & 0.3881\varepsilon_{t-3} + \varepsilon_t\end{aligned} \tag{3.4}$$

Equation (3.1) specifies ARIMA(5, 1, 5) as the most appropriate ARIMA model for inflation rate data. This is the model obtained through the OBB method. In Eq (3.2), ARIMA(5, 1, 2) represents the most appropriate ARIMA model for GDP growth rate, which is the model obtained from the OBB method. ARIMA(5, 1, 5) (similar to GDP growth rate but with different AR and MA parameter values) spelled out in Eq (3.3) is the model considered to be the most appropriate ARIMA model for interest rate data, which is the model developed from the OBB method. ARIMA(2, 1, 3) as stated in Eq (3.4) is the model selected as the most appropriate ARIMA model for unemployment rate data. This is the model obtained through the OBB method.

Each pair of Figures 16–19 presents line plot of error term, display of autocorrelation function (ACF) values of residuals, and the density plot/histogram of residuals. The plots of residual check is to enable one to know which model performs better among each pair. Each pair of Figure 16 illustrates residuals check for comparison of the model performance of the ARIMA model derived through the OBB (the proposed method) and CBB (the existing method) for inflation data. Each pair of Figure 17 shows residuals check for comparison of the model performance of the ARIMA model obtained through the OBB (the proposed method) and CBB (the existing method) for GDP growth rate. Each pair of Figure 18 illustrates residuals check for comparison of the model performance of the ARIMA model developed through the OBB (the proposed method) and CBB (the existing method) for interest rate data. Each pair of Figure 19 shows residuals check for comparison of the model performance of the ARIMA model obtained through the OBB (the proposed method) and CBB (the existing method) for unemployment data.

An eyesight inspection of each pair of line plot of the residuals presented in Figures 16–19 shows that none has a trend or pattern, rather each of them appears random in nature. Also, the ACF plots of each pair presented in Figures 16–19 shows that every coefficient lays within the 95% confidence

interval which suggests that every model from which the residual was obtained is a candidate of good ARIMA model to be fitted for is respective time series data. The point of focus is that the histogram plot of each pair of residual shows that the histogram of residual of the ARIMA model obtained from OBB methods looks more of bell-shape than each of their counterpart obtained from the CBB method for the four economic data of interest(the inflation rate, the GDP growth rate, the interest rate, and the unemployment rate data).

Having confirmed through the accuracy metrics of Table 8 and the model residual diagnostic plots of Figures 13–16 that the ACF of models obtained from the two methods confines within their confident limits for each economic data (the inflation rate, GDP growth rate, interest rate, and the unemployment rate), making each model a candidate of a good model for their respective series. Nevertheless, the shape of each histogram is examined to find out that histograms of error term obtained through the OBB (the proposed) method have a more bell-shape look than those obtained through CBB (the existing) method for every economic time series data considered.

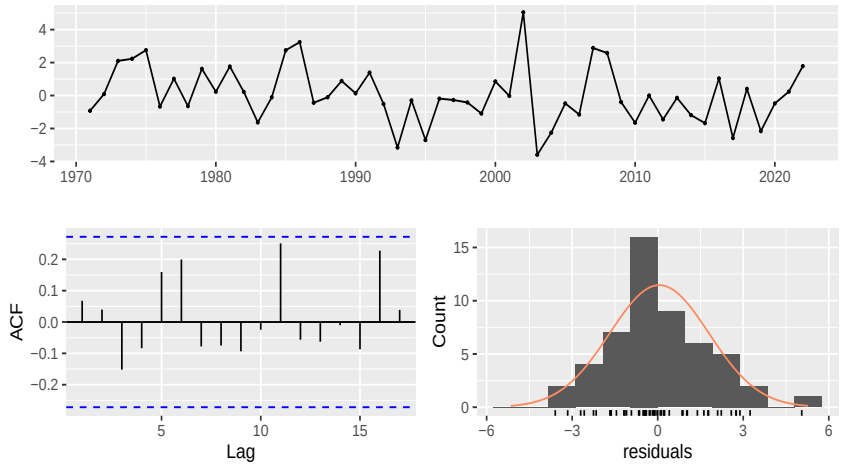

(a) Residuals check for OBB

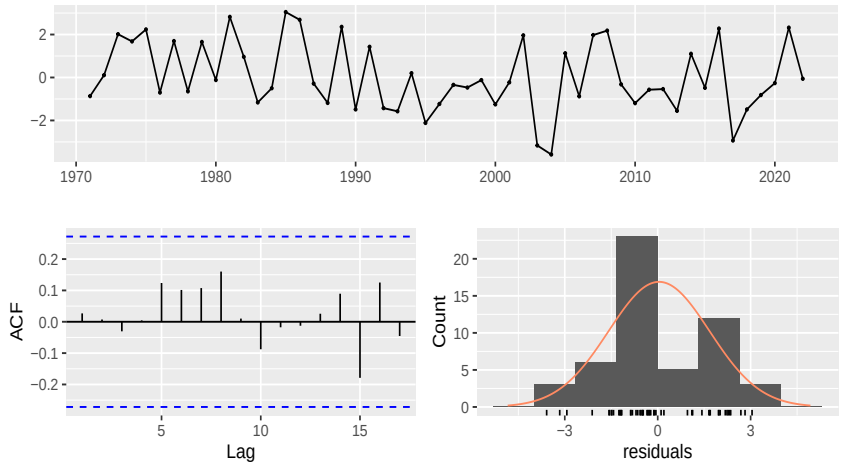

(b) Residuals check for CBB

Figure 16. Residuals analysis of inflation rate models using CBB and OBB methods.

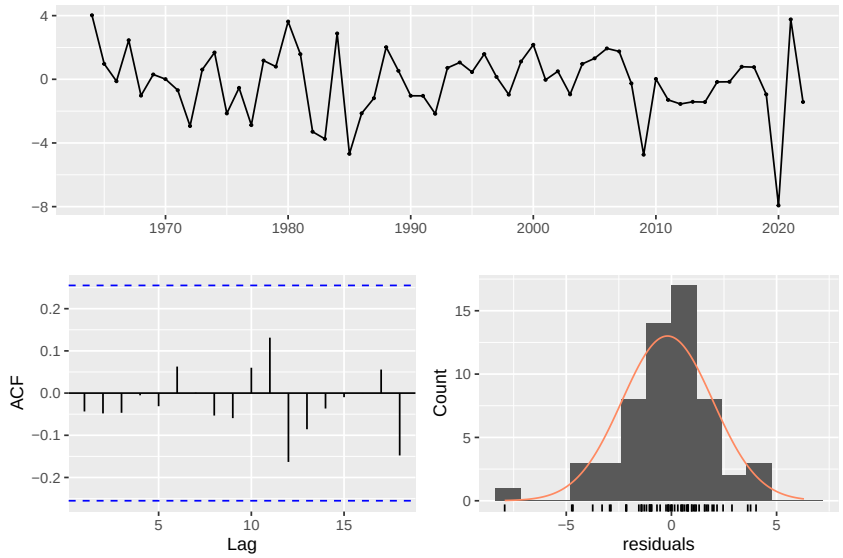

(a) Residuals check for OBB

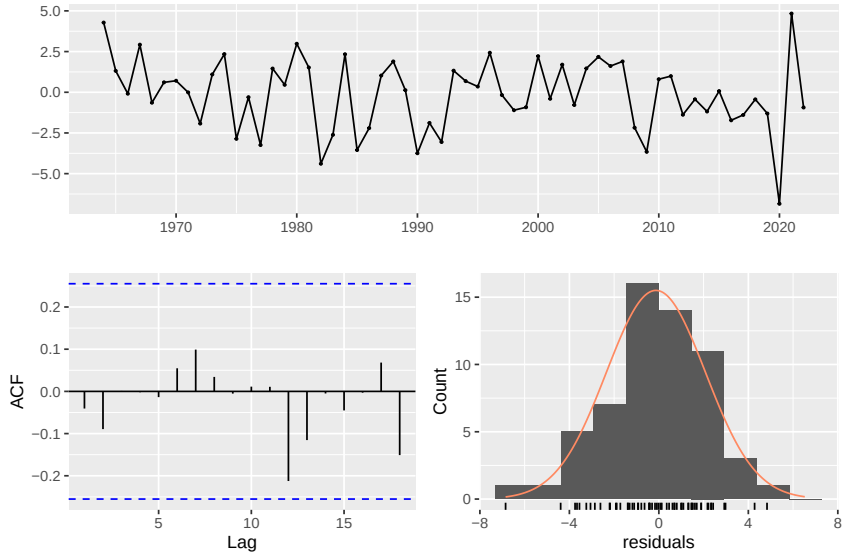

(b) Residuals check for CBB

Figure 17. Residuals analysis of the GDP models using CBB and OBB methods.

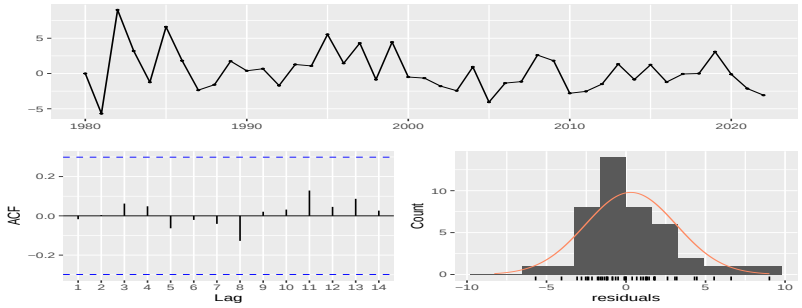

(a) Residuals check for OBB

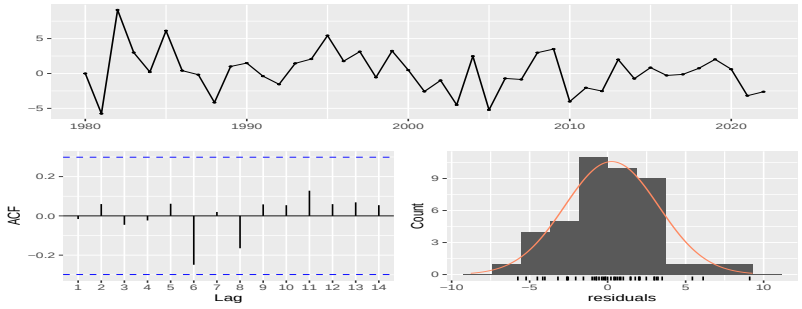

(b) Residuals check for CBB

Figure 18. Residuals analysis of the interest rate models using CBB and OBB methods.

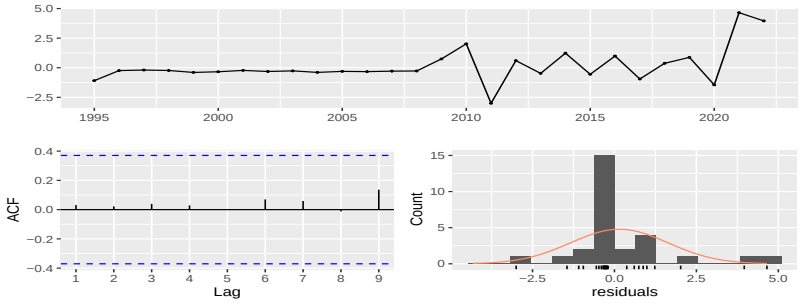

(a) Residuals check for OBB

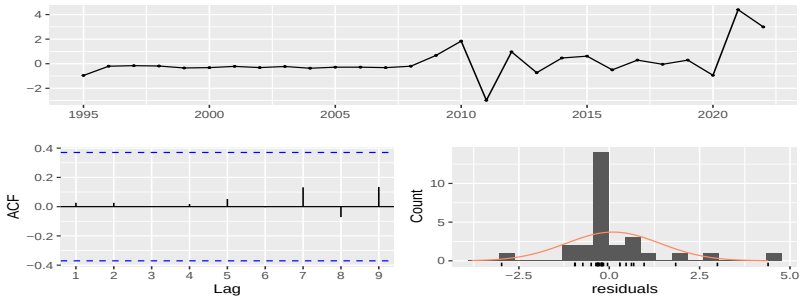

(b) Residuals check for CBB

Figure 19. Residuals analysis of the unemployment rate models using CBB and OBB methods.

Table 9. Forecast for the economic time series data using CBB and OBB methods.

Variable	Year	Method	Forecast	Lo_{80}	Hi_{80}	Lo_{95}	Hi_{95}
Inflation Rate	2023	CBB	7.816	5.272	10.360	3.925	11.707
		OBB	5.471	2.929	8.013	1.58	9.359
	2024	CBB	6.952	3.301	10.603	1.368	12.535
		OBB	4.979	1.259	8.699	−0.711	10.668
	2025	CBB	5.144	0.972	9.316	−1.237	11.524
		OBB	4.421	0.354	8.489	−1.800	10.642
	2026	CBB	4.437	−0.160	9.033	−2.594	11.467
		OBB	4.105	−0.147	8.357	−2.397	10.607
	2027	CBB	5.733	0.897	10.568	−1.663	13.128
		OBB	5.885	1.424	10.347	−0.938	12.709
GDP	2023	CBB	5.471	2.929	8.013	1.583	9.359
		OBB	0.587	−2.527	3.701	−4.175	5.349
	2024	CBB	4.979	1.259	8.699	−0.711	10.668
		OBB	−0.133	−3.315	3.049	−4.999	4.733
	2025	CBB	4.421	0.354	8.489	−1.800	10.642
		OBB	−0.312	−3.495	2.870	−5.179	4.556
	2026	CBB	4.105	−0.147	8.357	−2.397	10.607
		OBB	−1.780	−5.006	1.445	−6.714	3.153
	2027	CBB	5.885	1.424	10.347	−0.938	12.709
		OBB	−1.620	−4.998	1.758	−6.786	3.546
Interest Rate	2023	CBB	0.587	−2.527	3.701	−4.175	5.349
		OBB	1.653	−2.590	5.895	−4.836	8.141
	2024	CBB	−0.133	−3.315	3.049	−4.999	4.733
		OBB	1.311	−3.628	6.250	−6.243	8.864
	2025	CBB	−0.312	−3.495	2.870	−5.179	4.555
		OBB	2.391	−2.913	7.694	−5.720	10.501
	2026	CBB	−1.781	−5.006	1.445	−6.714	3.153
		OBB	3.659	−2.490	9.808	−5.745	13.063
	2027	CBB	−1.620	−4.998	1.758	−6.786	3.546
		OBB	2.973	−3.338	9.283	−6.678	12.624
Unempl-oyment Rate	2023	CBB	36.641	34.664	38.619	33.617	39.665
		OBB	36.529	34.544	38.514	33.494	39.564
	2024	CBB	38.900	35.541	42.259	33.763	44.037
		OBB	37.777	34.166	41.388	32.255	43.299
	2025	CBB	40.614	35.917	45.311	33.431	47.798
		OBB	40.349	35.381	45.316	32.752	47.945
	2026	CBB	40.252	33.939	46.564	30.597	49.906
		OBB	40.400	34.150	46.651	30.841	49.960
	2027	CBB	39.298	31.642	46.954	27.589	51.007
		OBB	40.567	32.867	48.267	28.791	52.342

Table 9 presents the forecast for each economic time series data and for each method (CBB and OBB) from 2023 to 2027.

4. Discussion

In this study, we introduced the OBB method, a novel approach to block bootstrapping that addresses some of the limitations of the traditional CBB method. The OBB method is designed to be more efficient, reduce overlap and variance, and improve statistical accuracy.

(a) The OBB method has been optimized to use fewer blocks than the CBB, leading to increased computational efficiency. This makes the OBB method particularly suitable for large datasets with limited computational resources.

(b) Our proposed method significantly improves the CBB by reducing the number of overlapping elements. This reduction in overlap contributes to the OBB method's overall performance in terms of variance and bias.

(c) The OBB method's design specifically targets the reduction of overlap, which are common issues in traditional block bootstrapping methods. By addressing these issues, the OBB method provides more reliable and accurate statistical estimates.

(d) The OBB method is tailored for applications where traditional block bootstrapping methods fall short. Its optimized design makes it particularly useful in scenarios requiring precise statistical inference with minimized error rates.

5. Conclusions

The OBB method significantly advances the performance of time series resampling techniques, especially in comparison to the CBB. By reducing block overlap and improving the efficiency of the resampling process, OBB captures temporal dependencies more effectively, leading to improved predictive accuracy and computational performance. In this study, OBB demonstrated superior results, achieving lower RMSE and lower MAE across ARMA models when applied to both simulated and real-world economic data. These reductions in error were consistent across various time series configurations, including key economic indicators such as inflation and GDP growth. OBB's flexibility in handling different block lengths and its capacity to maintain statistical accuracy across diverse datasets underscores its broad applicability. Future research should aim to extend the use of OBB to domain-specific applications such as financial forecasting and environmental modeling, further refining its capabilities and confirming its advantages in practical scenarios.

Author contributions

Daniel James: Conceptualization, Software, Formal analysis, Resources, Writing-original draft preparation, Writing-review and editing, Visualization, Funding acquisition; Kayode Ayinde: Methodology, Software, Formal analysis, Resources, Writing-original draft preparation, Writing-review and editing, Supervision, Funding acquisition; Adewale F. Lukman: Methodology, Resources,

Writing-original draft preparation, Writing-review and editing, Funding acquisition; Olayan Albalawi: Resources, Writing-original draft preparation, Writing-review and editing, Visualization, Funding acquisition; Jeza Allohibi: Resources, Writing-original draft preparation, Writing-review and editing, Visualization, Funding acquisition; Abdulmajeed A. Alharbi: Resources, Writing-original draft preparation, Writing-review and editing, Visualization, Funding acquisition. All authors have read and agreed to the published version of the manuscript.

Acknowledgments

We express our sincere gratitude to the editorial team and reviewers for their thorough review and valuable feedback, which have significantly improved the quality of our manuscript.

Conflict of interest

There is no conflict of interest.

References

1. K. Ayinde, J. Daniel, A. Adepetun, O. S. Ewemooje, Moving block bootstrap method with better elements representation for univariate time series data, *Reliability: Theory & Applications*, **18** (2023), 671–688. https://doi.org/10.24412/1932-2321-2023-374-671-688
2. P. Burridge, A. M. R. Taylor, Bootstrapping the HEGY seasonal unit root tests, *J. Econometrics*, **123** (2004), 67–87. https://doi.org/10.1016/j.jeconom.2003.10.029
3. E. Carlstein, The use of subseries values for estimating the variance of a general statistic from a stationary sequence, *Ann. Statist.*, **14** (1986), 1171–1179. https://doi.org/10.1214/aos/1176350057
4. T. Chai, R. R. Draxler, Root mean square error (RMSE) or mean absolute error (MAE), *Geosci. Model Dev. Discuss.*, **7** (2014), 1525–1534. https://doi.org/10.5194/gmdd-7-1525-2014
5. J. Daniel, K. Ayinde, OBL: optimum block length, package version 0.2.1, 2022. Available from: `https://CRAN.R-project.org/package=OBL`.
6. B. Efron, Bootstrap methods: another look at the jackknife, In: *Breakthroughs in statistics*, New York, NY: Springer, 1992, 569–593. https://doi.org/10.1007/978-1-4612-4380-9_41
7. P. Hall, Resampling a coverage pattern, *Stoch. Proc. Appl.*, **20** (1985), 231–246. https://doi.org/10.1016/0304-4149(85)90212-1
8. M. A. Hannan, D. N. T. How, M. S. H. Lipu, M. Mansor, P. J. Ker, Z. Y. Dong, et al., Deep learning approach towards accurate state of charge estimation for lithium-ion batteries using self-supervised transformer model, *Sci. Rep.*, **11** (2021), 19541. https://doi.org/10.1038/s41598-021-98915-8
9. T. Hesterberg, Bootstrap, *WIRS: Computational Statistics*, **3** (2011), 497–526. https://doi.org/10.1002/wics.182
10. J.-P. Kreiss, S. N. Lahiri, Bootstrap methods for time series, In: *Handbook of statistics*, Elsevier, **30** (2012), 3–26. https://doi.org/10.1016/B978-0-444-53858-1.00001-6

11. D. Kugiumtzis, Evaluation of surrogate and bootstrap tests for nonlinearity in time series, *Stud. Nonlinear Dyn. Econ.*, **12** (2008), 4. https://doi.org/10.2202/1558-3708.1474
12. H. R. Kunsch, The jackknife and the bootstrap for general stationary observations, *Ann. Statist.*, **17** (1989), 1217–1241. https://doi.org/10.1214/aos/1176347265
13. M. W. Liemohn, A. D. Shane, A. R. Azari, A. K. Petersen, B. M. Swiger, A. Mukhopadhyay, Rmse is not enough: guidelines to robust data-model comparisons for magnetospheric physics, *J. Atmos. Sol.-Terr. Phys.*, **218** (2021), 105624. https://doi.org/10.1016/j.jastp.2021.105624
14. R. Lyu, Y. Qu, K. Divaris, D. Wu, Methodological considerations in longitudinal analyses of microbiome data: a comprehensive review, *Genes*, **15** (2024), 51. https://doi.org/10.3390/genes15010051
15. T. Mathonsi, T. L. van Zyl, A statistics and deep learning hybrid method for multivariate time series forecasting and mortality modeling, *Forecasting*, **4** (2022), 1–25. https://doi.org/10.3390/forecast4010001
16. Macrotrends LLC, South Africa GDP Growth Rate 1961–2022, 2023. Available from: `https://www.macrotrends.net/countries/ZAF/south-africa/gdp-growth-rate`.
17. F. Petropoulos, E. Spiliotis, The wisdom of the data: getting the most out of univariate time series forecasting, *Forecasting*, **3** (2021), 478–497. https://doi.org/10.3390/forecast3030029
18. D. N. Politis, J. R. Romano, A circular block-resampling procedure for stationary data, Technical reports, Stanford University Department of Statistics, & National Science Foundation, 1991. Available from: `https://purl.stanford.edu/xh812zd4638`.
19. D. N. Politis, J. P. Romano, The stationary bootstrap, *J. Amer. Stat. Assoc.*, **89** (1994), 1303–1313. https://doi.org/10.1080/01621459.1994.10476870
20. M. R. Qader, S. Khan, M. Kamal, M. Usman, M. Haseeb, Forecasting carbon emissions due to electricity power generation in bahrain, *Environ. Sci. Pollut. Res.*, **29** (2022), 17346–17357. https://doi.org/10.1007/s11356-021-16960-2
21. B. Radovanov, A. Marcikić, A comparison of four different block bootstrap methods, *Croat. Oper. Res. Rev.*, **5** (2014), 189–202. https://doi.org/10.17535/crorr.2014.0007
22. W. J. Raseman, B. Rajagopalan, J. R. Kasprzyk, W. Kleiber, Nearest neighbor time series bootstrap for generating influent water quality scenarios, *Stoch. Environ. Res. Risk Assess.*, **34** (2020), 23–31. https://doi.org/10.1007/s00477-019-01762-3
23. X. Shao, The dependent wild bootstrap, *J. Amer. Stat. Assoc.*, **105** (2010), 218–235. https://doi.org/10.1198/jasa.2009.tm08744
24. K. Singh, On the asymptotic accuracy of efron's bootstrap, *Ann. Statist.*, **9** (1981), 1187–1195. https://doi.org/10.1214/aos/1176345636
25. K. Singh, M. Xie, Bootstrap: a statistical method, Rutgers University, USA, 2008. Available from: `https://statweb.rutgers.edu/mxie/RCPapers/bootstrap.pdf`.
26. The R Core Team, The R Project for Statistical Computing, 2022. Available from: `https://www.r-project.org/`.
27. H. D. Vinod, New bootstrap inference for spurious regression problems, *J. Appl. Stat.*, **43** (2016), 317–335. https://doi.org/10.1080/02664763.2015.1049939

28. S. Wang, Y. Fan, S. Jin, P. Takyi-Aninakwa, C. Fernandez, Improved anti-noise adaptive long short-term memory neural network modeling for the robust remaining useful life prediction of lithium-ion batteries, *Reliab. Eng. Syst. Safe.*, **230** (2023), 108920. https://doi.org/https://doi.org/10.1016/j.ress.2022.108920

29. S. Wang, F. Wu, P. Takyi-Aninakwa, C. Fernandez, D.-I. Stroe, Q. Huang, Improved singular filtering-gaussian process regression-long short-term memory model for whole-life-cycle remaining capacity estimation of lithium-ion batteries adaptive to fast aging and multi-current variations, *Energy*, **284** (2023), 128677. https://doi.org/10.1016/j.energy.2023.128677

30. Y. Wang, New developments in sequential change point detection for time series and spatio-temporal analysis, PhD thesis, University of Connecticut, 2023.

31. A. Young, Consistency without inference: instrumental variables in practical application, *Eur. Econ. Rev.*, **147** (2022), 104112. https://doi.org/10.1016/j.euroecorev.2022.104112

32. G. A. Young, Bootstrap: More than a stab in the dark?, *Statist. Sci.*, **9** (1994), 382–395. https://doi.org/10.1214/ss/1177010383

AIMS Press